

A Genuinely Multidimensional High-Resolution Scheme for the Elastic–Plastic Wave Equation

Guido Giese and Michael Fey

Seminar for Applied Mathematics, Swiss Federal Institute of Technology, Zurich, Switzerland

Received February 6, 2002; revised June 3, 2002

In this paper we present a numerical method of high order for solving the multidimensional elastic–plastic wave equation. The basic idea is to decompose the hyperbolic PDE into advection equations, which can be solved numerically. Furthermore, the occurrence of plasticity makes it necessary to solve an ODE for the stress–strain relationship at every point. © 2002 Elsevier Science (USA)

1. INTRODUCTION

The wave equation of an elastic material represents a hyperbolic conservation law for the momentum and the strain variables and can be solved with standard methods for conservation laws. However, for solids which undergo plastic deformation, only the momentum but not the strain variables are conserved.

There exist a large number of numerical schemes for hyperbolic equations (cf. [1, 4, 7, 8, 19]), some of which have been used for the simulation of waves in solids (e.g., [9]–[14]). In this work, we follow the ansatz of Fey *et al.* in [2, 3, 5], who developed a high-order scheme called Method of Transport for solving multidimensional Euler equations. The basic idea is to decompose the partial differential equation into scalar advection equations which can be solved numerically.

Although the elastic–plastic wave equation is not a pure conservation law, we were able to use the ansatz of Fey to construct a genuinely multidimensional numerical scheme of high order for plastic waves. It is important to mention that unlike most other numerical schemes, our method can be used for approximations of any order in space and time, which is extremely advantageous for simulations of high accuracy. Furthermore, the general treatment of elasto-plasticity introduced in this paper can be used for other numerical methods for hyperbolic PDEs as well and for any kind of hysteresis model. For example, a treatment of hysteresis effects in electrodynamics would be straightforward with the numerical concepts presented.

In this paper we first give a brief introduction into the governing equations of elasto-plasticity. Afterward, we present our numerical scheme and finally we give some numerical results in 2-D and 3-D.

2. GOVERNING EQUATIONS

We use a formulation of the elastic-plastic wave equation as a first-order system, which means we have to use three physical variables: The symmetric stress tensor $\underline{\sigma}$, the symmetric strain tensor $\underline{\epsilon}$, and the velocity vector \vec{v} . Furthermore, we need the deviatoric stress tensor \underline{s} , which is defined as $s_{ij} = \sigma_{ij} - \frac{1}{3}\delta_{ij}\sigma_{kk}$.

With these variables, we get three equations describing the conservation of momentum ($\rho = \text{density}$)

$$\rho \frac{\partial}{\partial t} v_i = \sum_{j=1}^3 \frac{\partial}{\partial x_j} \sigma_{ij} \quad i = 1, \dots, 3 \quad (1)$$

and six compatibility relations between velocity and strain variables

$$\frac{\partial}{\partial t} \epsilon_{ij} = \frac{1}{2} \left(\frac{\partial}{\partial x_j} v_i + \frac{\partial}{\partial x_i} v_j \right) \quad i \leq j = 1, \dots, 3, \quad (2)$$

which are due to the fact that both strain and velocity variables are derivatives of the displacement vector \vec{u} . Altogether we obtain nine equations describing wave phenomena in solids. However, we still need an equation connecting stress and strain variables. For plasticity there exists a relationship between infinitesimal changes of stress and strain only (cf. [18]),

$$\frac{\partial}{\partial t} \epsilon_{ij} = \frac{1+\nu}{E} \frac{\partial}{\partial t} \sigma_{ij} - \frac{\nu}{E} \delta_{ij} \frac{d}{dt} \sigma_{kk} + s_{ij} \frac{d}{dt} \chi, \quad (3)$$

with $\nu = \text{Poisson's ratio}$ and $E = \text{Young's modulus}$. For elasticity Eq. (3) reduces with $\frac{d}{dt} \chi \equiv 0$ to Hooke's law. It has to be mentioned that our system describes solids in the limit of small strains; i.e., it is a linearization of the general flow equations (cf. [6, 15]).

To distinguish between elastic and plastic deformation we use the so-called von Mises yield function:

$$f(\underline{\mathbf{g}}) = \frac{1}{2} s_{ij} s_{ij} =: \kappa^2. \quad (4)$$

Basically, plasticity occurs at a certain point if the current function $\kappa(t)$ in that point attains the value of $\kappa_0(t)$, which is the maximal value of $\kappa(t)$ in the past; i.e., with

$$\kappa_0(t) = \max_{t_0 \leq t' \leq t} \kappa(t')$$

three different cases may occur:

- $\kappa(t) < \kappa_0(t)$: Elastic deformation.
- $\kappa(t) = \kappa_0(t)$ and $\frac{d}{dt} \kappa \leq 0$: Elastic deformation.
- $\kappa(t) = \kappa_0(t)$ and $\frac{d}{dt} \kappa > 0$: Plastic deformation.

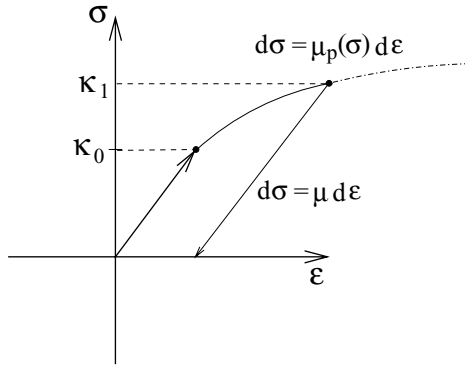


FIG. 1. Response of the strain variable ϵ to the stress σ in the case when hysteresis occurs: For small stresses (i.e., $|\sigma| \leq \kappa_0$), the relationship is linear (Hooke’s law). However, if the stress $|\sigma|$ exceeds a certain value κ_0 then plastic flow occurs. Furthermore, unloading processes are always assumed to be elastic in our plasticity model. After the plastic loading and the elastic unloading process, plasticity will occur again if $|\sigma| \geq \kappa_1$ with κ_1 being the largest value of the stress $|\sigma|$ in the past.

This plasticity model reduces to the well-known hysteresis curve as shown in Fig. 1 in the case of one stress and one strain variable.

Furthermore, for this yield criterion the function $\frac{d}{dt} \chi$ from Eq. (3) can be written in the form

$$\frac{d}{dt} \chi = \frac{1}{2\kappa} \left(\frac{1}{\mu_p(\kappa)} - \frac{1}{\mu} \right) \frac{d}{dt} \kappa, \tag{5}$$

with a measured function $\mu_p(\kappa) \leq \mu$ (cf. Fig. 1) and the elastic shear modulus $\mu = \frac{E}{2(1+\nu)}$. Hence, we have a system of the form

$$\mathbf{V}_t + \nabla \cdot \mathbf{c} \underline{\mathbf{L}}(\mathbf{U}) = 0 \quad (c = \text{wave speed, to be specified later}) \tag{6}$$

$$\underline{\boldsymbol{\sigma}}_t = \underline{\mathbf{C}}(\boldsymbol{\sigma}) : \underline{\boldsymbol{\epsilon}}_t, \tag{7}$$

where we defined the vectors

$$\mathbf{V} = (v_1, v_2, v_3, \epsilon_{11}, \epsilon_{22}, \epsilon_{33}, \epsilon_{12}, \epsilon_{13}, \epsilon_{23})^T \tag{8}$$

$$\mathbf{U} = (v_1, v_2, v_3, \sigma_{11}, \sigma_{22}, \sigma_{33}, \sigma_{12}, \sigma_{13}, \sigma_{23})^T. \tag{9}$$

Equation (6) summarizes the conservation of momentum (1) and the compatibility relations (2) ($\underline{\mathbf{L}}(\mathbf{U})$ is a linear function of \mathbf{U} , since both equations are linear) and Eq. (7) contains the stress–strain relationship from (3) with the rank-4 tensor $\underline{\mathbf{C}}(\boldsymbol{\sigma})$.

Thus, the governing equation consists of a flux equation (6) and an ODE (7) at every point. Theoretically, one could use Eq. (7) to replace the time derivatives of the strains by time derivatives of the stresses in Eq. (6) to come to a closed form of a PDE. However, numerically it turns out to be advantageous to solve these two parts of the physical system separately, except for the case of elasticity (i.e., no plasticity is allowed in general), where $\underline{\mathbf{C}}(\boldsymbol{\sigma})$ is constant and hence the closed form of the system is a linear conservation law. One of the main problems in the plastic case—which can only be treated numerically by splitting the system into a PDE and an ODE at every point—is the fact that the matrix $\underline{\mathbf{C}}(\boldsymbol{\sigma})$ can

be discontinuous at the transition from elasticity to plasticity in a point and thus the exact transition point has to be found by iteration (cf. below).

The most important difference between the elastic wave equation and the standard wave equation $\phi_{tt} - c^2 \Delta \phi = 0$ is the existence of several wave modes. In the elastic case there are compression waves with wave speed

$$c_1 = \sqrt{\frac{K + 4/3\mu}{\rho}}$$

(with bulk modulus $K = \frac{E}{3(1-2\nu)}$) and shear waves with wave speed

$$c_2 = \sqrt{\frac{\mu}{\rho}} < c_1.$$

In plastic regions we find an additional fast plastic wave c_f and a slow plastic wave c_s with $c_s < c_2 < c_f < c_1$ (cf. [9, 17]).

3. NUMERICAL SCHEME

Due to the structure of Eqs. (6) and (7) our numerical scheme consists of two steps:

1. Solve flux equation (6) with a solver for hyperbolic PDEs. We use the Method of Transport in the following.
2. Integrate the stress-strain relationship (7) in time for every cell of the grid with a high-order ODE solver.

We will now discuss both steps in detail.

3.1. The Method of Transport

The basic idea of the Method of Transport is to rewrite flux equation (6) equivalently as a coupled system of advection equations. Therefore, we introduce a set of direction vectors $\vec{n}_i, i = 1, \dots, k$ which have to fulfill the following two consistency relations:

$$\sum_{i=1}^k \vec{n}_i = 0, \quad \frac{1}{k} \sum_{i=1}^k \vec{n}_i \vec{n}_i^T = \underline{I}. \quad (10)$$

With these definitions we can rewrite the flux equation as follows:

$$\mathbf{V}_t + \nabla \cdot c \underline{\mathbf{L}} = 0 \quad (11)$$

$$\Leftrightarrow \frac{1}{k} \sum_{i=1}^k \{ (\mathbf{V} + \underline{\mathbf{L}} \vec{n}_i)_t + \nabla \cdot c (\mathbf{V} + \underline{\mathbf{L}} \vec{n}_i) \vec{n}_i^T \} = 0. \quad (12)$$

We observe that our flux equation can be written as a system of coupled advection equations, each of which transports the quantity $\frac{1}{k} (\mathbf{V} + \underline{\mathbf{L}} \vec{n}_i)$ at the velocity $c \vec{n}_i$.

Note that Eq. (12) is strictly equivalent to the original equation (11). Our approximation consists of decoupling the system; i.e., at a certain time step t^n we define the independent

quantities

$$\mathbf{R}_i(\vec{x}, t^n) := \frac{1}{k}(\mathbf{V}(\vec{x}, t^n) + \mathbf{L}(\vec{x}, t^n)\vec{n}_i) \quad (13)$$

and then solve the advection equations

$$(\mathbf{R}_i)_t + \nabla \cdot (\mathbf{R}_i c \vec{n}_i^T) = 0 \quad \forall i \quad (14)$$

independently on the time interval $I = [t^n, t^{n+1}]$. At the next time step t^{n+1} the update for the vector \mathbf{V} reads.

$$\mathbf{V}(\vec{x}, t^{n+1}) = \sum_{i=1}^k \mathbf{R}_i(\vec{x}, t^{n+1}). \quad (15)$$

This yields a first-order approximation for the exact solution in time if consistency relations (10) hold, since

$$\mathbf{V}_t = \sum_{i=1}^k (\mathbf{R}_i)_t = - \sum_{i=1}^k \nabla \cdot (c \mathbf{R}_i \vec{n}_i^T) = -\nabla \cdot c \mathbf{L}.$$

However, to obtain approximations of higher order in time one has to add correction terms into the numerical fluxes, i.e., one uses slightly modified quantities in the advection equations

$$\mathbf{R}_i := \frac{1}{k}(\mathbf{V} + (\mathbf{L} + \mathbf{K})\vec{n}_i),$$

where the correction matrix \mathbf{K} can be found by comparing the Taylor expansion of the exact solution to the expansion of the numerical scheme, which we show for the 2-D case (i.e., $\vec{x} = (x, y)^T$) in the following (the 3-D case is analogous). The derivation of the correction terms is quite similar to the derivation of the second-order Lax–Wendroff scheme (cf. [16]).

For the exact solution of Eq. (6) we obtain

$$\mathbf{V}(\vec{x}, t_0 + \Delta t) = \mathbf{V}(\vec{x}, t_0) + \Delta t \mathbf{V}_t(\vec{x}, t_0) + \frac{\Delta t^2}{2} \mathbf{V}_{tt}(\vec{x}, t_0) + \dots$$

Flux equation (6) in 2-D can be rewritten in the form (since it is linear)

$$\mathbf{V}_t = \mathbf{A} \mathbf{U}_x + \mathbf{B} \mathbf{U}_y$$

with two constant matrices \mathbf{A} and \mathbf{B} . Taking into account the definition of \mathbf{V} and \mathbf{U} (Eqs. (8) and (9)) and the stress–strain relationship (3) it is straightforward to see that a linear relationship of the form

$$\mathbf{U}_t = \mathcal{A}(\boldsymbol{\sigma}) \mathbf{V}_t \quad (16)$$

exists with a matrix \mathcal{A} .

Now, we can easily replace derivatives in time by spatial derivatives:

$$\mathbf{V}_t = \underline{\mathbf{A}}\mathbf{U}_x + \underline{\mathbf{B}}\mathbf{U}_y = \nabla \cdot [\underline{\mathbf{A}}\mathbf{U}, \underline{\mathbf{B}}\mathbf{U}] \quad (17)$$

$$\begin{aligned} \mathbf{V}_{tt} &= \underline{\mathbf{A}}(\mathbf{U}_t)_x + \underline{\mathbf{B}}(\mathbf{U}_t)_y \\ &= \nabla \cdot \{[\underline{\mathbf{A}}, \underline{\mathbf{B}}](\underline{\mathbf{A}}(\underline{\boldsymbol{\sigma}})\mathbf{V}_t)\} \end{aligned} \quad (18)$$

$$=: \nabla \cdot \underline{\mathbf{Z}}. \quad (19)$$

The Taylor expansion of advection equation (14) is

$$\mathbf{R}_i(\vec{\mathbf{x}}, t_0 + \Delta t) = \mathbf{R}_i(\vec{\mathbf{x}}, t_0) + \Delta t(\mathbf{R}_i)_t(\vec{\mathbf{x}}, t_0) + \frac{\Delta t^2}{2}(\mathbf{R}_i)_{tt}(\vec{\mathbf{x}}, t_0) + \dots \quad (20)$$

Using advection equation (14), time derivatives can be replaced by spatial derivatives:

$$\begin{aligned} (\mathbf{R}_i)_t &= -\nabla \cdot (\mathbf{R}_i \vec{\mathbf{n}}_i^T c) \\ (\mathbf{R}_i)_{tt} &= -\nabla \cdot ((\mathbf{R}_i)_t \vec{\mathbf{n}}_i^T c) = \nabla \cdot ((\nabla \cdot (\mathbf{R}_i \vec{\mathbf{n}}_i^T c)) \vec{\mathbf{n}}_i^T c). \end{aligned} \quad (21)$$

Obviously, our scheme is first-order accurate since

$$\begin{aligned} \sum_{i=1}^k \mathbf{R}_i(\vec{\mathbf{x}}, t_0) &= \mathbf{V}(\vec{\mathbf{x}}, t_0) \\ \sum_{i=1}^k \mathbf{R}_i(\vec{\mathbf{x}}, t_0) \vec{\mathbf{n}}_i^T c &= c \underline{\mathbf{L}}, \end{aligned}$$

which gives

$$\sum_{i=1}^k (\mathbf{R}_i)_t(\vec{\mathbf{x}}, t_0) = \mathbf{V}_t(\vec{\mathbf{x}}, t_0) = -\nabla \cdot c \underline{\mathbf{L}}(\vec{\mathbf{x}}, t_0) = -\sum_{i=1}^k \nabla \cdot (\mathbf{R}_i(\vec{\mathbf{x}}, t_0) \vec{\mathbf{n}}_i^T c). \quad (22)$$

However, comparing Eq. (17) to Eq. (21) it turns out that the second-order derivatives in time are not the same,

$$\mathbf{V}_{tt} - \sum_{i=1}^k (\mathbf{R}_i)_{tt} = \nabla \cdot \left(\underline{\mathbf{Z}} + \sum_{i=1}^k (\mathbf{R}_i)_t \vec{\mathbf{n}}_i^T c \right) = \nabla \cdot \underline{\mathbf{K}} \neq 0, \quad (23)$$

with $\underline{\mathbf{K}} := \underline{\mathbf{Z}} + \sum_{i=1}^k (\mathbf{R}_i)_t \vec{\mathbf{n}}_i^T c$. We define the correction matrix \mathbf{K} by

$$\underline{\mathbf{K}} = \frac{\Delta t}{2} \mathbf{K} \quad (24)$$

and the transported quantities $\tilde{\mathbf{R}}_i$ by

$$\tilde{\mathbf{R}}_i := \frac{1}{k} \left(\mathbf{V} + \left(\underline{\mathbf{L}} + \frac{1}{c} \underline{\mathbf{K}} \right) \vec{\mathbf{n}}_i \right). \quad (25)$$

Equation (22) still holds for the $\tilde{\mathbf{R}}_i$ (\Rightarrow the scheme is still consistent). Furthermore, one can easily verify

$$\sum_{i=1}^k (\tilde{\mathbf{R}}_i)_t(\vec{x}, t_0) = \sum_{i=1}^k (\mathbf{R}_i)_t(\vec{x}, t_0) - \frac{\Delta t}{2} \nabla \cdot \tilde{\mathbf{K}} \quad (26)$$

and consequently

$$\mathbf{V}(\vec{x}, t_0 + \Delta t) - \sum_{i=1}^k \tilde{\mathbf{R}}_i(\vec{x}, t_0 + \Delta t) = \mathcal{O}(\Delta t^3).$$

Our decomposition is now of second order, since the second-order error (23) is compensated by the correction term appearing in the first-order derivative of $\tilde{\mathbf{R}}_i$. Third and fourth order can be achieved analogously.

The integration of the decoupled advection equations (14) can be written in a simple explicit form, since the wave speed c is constant:

$$\mathbf{R}_i(\vec{y}, t) = \int_{\mathbf{R}^2} \mathbf{R}_i(\vec{x}, t^n) \delta(\vec{y} - [\vec{x} + c\vec{n}_i \Delta t]) d\vec{x}. \quad (27)$$

The question arises as to what wave speed we must choose for c . Any choice of c would give us a consistent scheme but for stability reasons (CFL-condition) the numerical wave speed has to be greater to or equal to the physical wave speed. For that reason, we choose in elastic and plastic regions the greatest possible physical wave speed, (i.e., $c = c_1$) as the speed to advect the quantities \mathbf{R}_i .

So far our discussion has been semidiscrete only since we have not discretized the space variables yet. The space discretization can be performed as for all types of finite volume methods; i.e., one has to add the following two steps:

- At a certain time level one computes cell averages for each cell I_{ij} (we assumed a grid in 2-D) for the quantity \mathbf{V} according to Eq. (15):

$$\bar{\mathbf{V}}_{ij}^{n+1} = \frac{1}{|I_{ij}|} \sum_{l=1}^k \int_{I_{ij}} \mathbf{R}_l(\vec{y}, t^{n+1}) d\vec{y}.$$

- Before each time step one has to reconstruct the function $\mathbf{V}(\vec{x}, t)$ by polynomials in space from the previously updated cell averages.

It is important to mention that any wave model fulfilling conditions (10) will lead to a consistent numerical scheme. The simplest models (in 2-D) which can be found are the four diagonal propagation directions (i.e., $k = 4$):

$$\vec{n}_1 = \begin{pmatrix} 1 \\ 1 \end{pmatrix}, \quad \vec{n}_2 = \begin{pmatrix} 1 \\ -1 \end{pmatrix}, \quad \vec{n}_3 = \begin{pmatrix} -1 \\ 1 \end{pmatrix}, \quad \vec{n}_4 = \begin{pmatrix} -1 \\ -1 \end{pmatrix}. \quad (28)$$

However, to obtain good numerical results it is important to take into account more physical information to choose an appropriate wave model. For this reason, we chose a wave model for the decomposition of our 2-D or 3-D wave equation, which reduces automatically to the decomposition into right eigenvectors for an elastic 1-D problem, which we know is exact in 1-D, which means that if we simulate a 1-D problem, along the x - or y -axis with our

multidimensional scheme it will be equivalent to the transport of right eigenvectors at the speed of the eigenvalues of the Jacobian matrix in 1-D. An example of such a wave model in 2-D will be presented in the next section.

To conclude, the Method of Transport yields an update for the vector \mathbf{V} which is high-order in time due to the use of correction terms and high order in space by using a polynomial reconstruction in each cell.

3.2. Choice of a Wave Model for Plane Strain

As mentioned in the previous section, the choice of the wave model \vec{n}_i plays an important role in achieving good numerical results. Hence, to take into account the physical behavior of the system, we require our multidimensional decomposition to reduce to the exact 1-D decomposition into right eigenvectors if we simulate a linear 1-D problem with our multidimensional scheme.

We demonstrate this argument for the 2-D case of a solid under so-called plane-strain waves; i.e., the z -component of the displacement and velocity vector is vanishing:

$$\epsilon_{33} = \sigma_{23} = \sigma_{13} = v_3 \equiv 0. \quad (29)$$

We start our discussion with the wave model for elasticity and then transfer the results to plastic waves. For elasticity the ODE (7) is trivial since $\underline{\mathbf{C}}(\boldsymbol{\sigma})$ is constant. Thus, we can plug Eq. (7) and condition (29) into Eq. (6) and obtain the wave equation in 2-D for plane strain (closed form),

$$\begin{pmatrix} v_1 \\ v_2 \\ \sigma_{11} \\ \sigma_{22} \\ \sigma_{33} \\ \sigma_{12} \end{pmatrix}_t = \nabla \cdot \begin{pmatrix} \frac{1}{\rho}\sigma_{11} & \frac{1}{\rho}\sigma_{12} \\ \frac{1}{\rho}\sigma_{12} & \frac{1}{\rho}\sigma_{22} \\ v_1(K + \frac{4}{3}\mu) & v_2(K - \frac{2}{3}\mu) \\ v_1(K - \frac{2}{3}\mu) & v_2(K + \frac{4}{3}\mu) \\ v_2(K - \frac{2}{3}\mu) & v_2(K - \frac{2}{3}\mu) \\ v_2\mu & v_1\mu \end{pmatrix}, \quad (30)$$

with the Bulk modulus $K = \frac{E}{3(1-2\nu)}$. For our multidimensional decomposition we will use a combination of the right eigenvectors for the x - and y -directions, which takes into account the propagation of transverse waves at speed c_2 and longitudinal waves at speed c_1 . At first, we remember that for any linear conservation law in 1-D

$$\mathbf{U}_t + \underline{\mathbf{A}}\mathbf{U}_x = 0$$

the exact solution just advects right eigenvectors of the matrix $\underline{\mathbf{A}}$ at the speed of its eigenvalues (cf.[8]). Thus, we have a look at the eigenvectors which are transported by 1-D waves along the x - and y -axes. Table (I) summarizes the result.

The equation has four nontrivial eigenvalues $\pm c_1$ for longitudinal waves and $\pm c_2$ for shear waves.

Now, we want our multidimensional decomposition into advection equations to transport exactly these eigenvectors if we simulate a 1-D problem, which means that our 2-D

TABLE I
Decomposition of the 1-D Elastic Wave Equation into Right Eigenvectors
 $U = \sum_i R_i$ Along the x - and y -axes

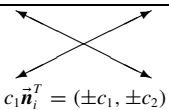
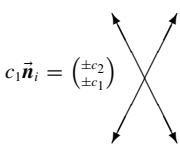
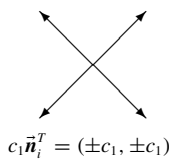
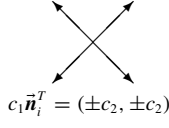
Eigenvalue of Jacobian	R_i in x -direction	R_i in y -direction
$\pm c_1$	$\begin{pmatrix} \frac{1}{2} \left(v_1 \pm \frac{\sigma_{11}}{\rho c_1} \right) \\ 0 \\ \frac{1}{2} (v_1 \rho c_1 \pm \sigma_{11}) \\ \frac{1}{2} \left(\frac{v_1}{\rho c_1} \pm \sigma_{11} \frac{K-2/3\mu}{K+4/3\mu} \right) \\ \frac{1}{2} \left(\frac{v_1}{c_1} \pm \sigma_{11} \frac{K-2/3\mu}{K+4/3\mu} \right) \\ 0 \end{pmatrix}$	$\begin{pmatrix} 0 \\ \frac{1}{2} \left(v_2 \pm \frac{\sigma_{22}}{\rho c_1} \right) \\ \frac{1}{2} \left(\frac{v_2}{c_1} \pm \sigma_{22} \frac{K-2/3\mu}{K+4/3\mu} \right) \\ \frac{1}{2} (v_2 \rho c_1 \pm \sigma_{22}) \\ \frac{1}{2} \left(\frac{v_2}{c_1} \pm \sigma_{22} \frac{K-2/3\mu}{K+4/3\mu} \right) \\ 0 \end{pmatrix}$
$\pm c_2$	$\begin{pmatrix} 0 \\ \frac{v_2}{2} \pm \frac{\sigma_{12}}{2\rho c_2} \\ 0 \\ 0 \\ 0 \\ \frac{\sigma_{12}}{2} \pm \frac{v_2 \rho c_2}{2} \end{pmatrix}$	$\begin{pmatrix} \frac{v_1}{2} \pm \frac{\sigma_{12}}{2\rho c_2} \\ 0 \\ 0 \\ 0 \\ 0 \\ \frac{\sigma_{12}}{2} \pm \frac{v_1 \rho c_2}{2} \end{pmatrix}$
0	$\begin{pmatrix} 0 \\ 0 \\ 0 \\ \sigma_{22} - \frac{K-2/3\mu}{K+4/3\mu} \sigma_{11} \\ 0 \\ 0 \end{pmatrix}$	$\begin{pmatrix} 0 \\ 0 \\ \sigma_{11} - \frac{K-2/3\mu}{K+4/3\mu} \sigma_{22} \\ 0 \\ 0 \\ 0 \end{pmatrix}$
0	$\begin{pmatrix} 0 \\ 0 \\ 0 \\ 0 \\ \sigma_{33} - \frac{K-2/3\mu}{K+4/3\mu} \sigma_{11} \\ 0 \end{pmatrix}$	$\begin{pmatrix} 0 \\ 0 \\ 0 \\ 0 \\ \sigma_{33} - \frac{K-2/3\mu}{K+4/3\mu} \sigma_{22} \\ 0 \end{pmatrix}$

numerical scheme reduces to the exact 1-D decomposition automatically. Therefore, we have to use a different wave model for each component of Eq. (30); i.e., in each component we transport the physical quantities (from Table I) with the “correct” physical speed along the x - and y -axes (cf. Table II). Hence, at this point we generalize Fey’s concept (cf. [2, 3]) of decomposing a PDE into advection equations presented in Eq. (13) in such a way that each component of the state vector \mathbf{V} and the flux matrix (\mathbf{L} is decomposed and advected with a different wave model \vec{n}_i).¹ However, the algorithms for solving the advection equations and calculating correction terms for high order presented above stay the same.

¹ To be mathematically correct one has to use a second index j for the wave model \vec{n}_i^j , denoting the component j of the PDE that it is used for. For the following example focusing on one component of the PDE this index is omitted.

TABLE II

Decomposition of the Elastic Wave Equation in 2-D into Advection Equations

Equation	Transported quantity $\times 4$	Wave model
$\frac{\partial v_1}{\partial t} = \nabla \cdot \left(\frac{\sigma_{11}}{\rho}, \frac{\sigma_{12}}{\rho} \right)$	$v_1 - \left(\frac{1}{c_1} \frac{\sigma_{11}}{\rho}, \frac{c_1}{c_2^2} \frac{\sigma_{12}}{\rho} \right) \vec{n}_i$	 $c_1 \vec{n}_i^T = (\pm c_1, \pm c_2)$
$\frac{\partial v_2}{\partial t} = \nabla \cdot \left(\frac{\sigma_{12}}{\rho}, \frac{\sigma_{22}}{\rho} \right)$	$v_2 - \left(\frac{c_1}{c_2^2} \frac{\sigma_{12}}{\rho}, \frac{1}{c_1} \frac{\sigma_{22}}{\rho} \right) \vec{n}_i$	 $c_1 \vec{n}_i = \begin{pmatrix} \pm c_2 \\ \pm c_1 \end{pmatrix}$
$\frac{\partial \sigma_{11}}{\partial t} = \nabla \cdot (a v_1, b v_2)$	$\sigma_{11} - \frac{1}{c_1} (a v_1, b v_2) \vec{n}_i$	 $c_1 \vec{n}_i^T = (\pm c_1, \pm c_1)$
$\frac{\partial \sigma_{22}}{\partial t} = \nabla \cdot (b v_1, a v_2)$	$\sigma_{22} - \frac{1}{c_1} (b v_1, a v_2) \vec{n}_i$	
$\frac{\partial \sigma_{33}}{\partial t} = \nabla \cdot (b v_1, b v_2)$	$\sigma_{33} - \frac{1}{c_1} (b v_1, b v_2) \vec{n}_i$	
$\frac{\partial \sigma_{12}}{\partial t} = \nabla \cdot (\mu v_2, \mu v_1)$	$\sigma_{12} - \frac{1}{c_2} (\mu v_2, \mu v_1) \vec{n}_i$	 $c_1 \vec{n}_i^T = (\pm c_2, \pm c_2)$

Notes. For each component of the equation (left column) a different wave model is used (right column). The transported quantities (i.e., the vectors \mathbf{R}_i) are indicated in the middle column componentwise (the factor 1/4 is omitted). The advection equations for this multidimensional decomposition reduces to the 1-D decomposition into right eigenvectors along the x - and y -axes. $a = K + 4/3\mu$; $b = K - 2/3\mu$.

As an example, we demonstrate our argument for the first component of system (30). A 1-D wave along the x -axis transports the quantity $\frac{1}{2}(v_1 \pm \frac{\sigma_{11}}{\rho c_1})$ at speed $\pm c_1$ along the x -axis, whereas a 1-D wave along the y -axis transports the quantity $\frac{1}{2}(v_1 \pm \frac{\sigma_{12}}{\rho c_2})$ at speed $\pm c_2$ along the y -axis in the first component of the system (cf. first and second row of Table I). Our multidimensional scheme indicated in Table II now contains for the first component of the system the advection equations

$$\frac{1}{4} \left(v_1 - \left(\frac{1}{c_1} \frac{\sigma_{11}}{\rho}, \frac{c_1}{c_2^2} \frac{\sigma_{12}}{\rho} \right) \vec{n}_i \right)_t + \nabla \cdot \left(\frac{1}{4} \left(v_1 - \left(\frac{1}{c_1} \frac{\sigma_{11}}{\rho}, \frac{c_1}{c_2^2} \frac{\sigma_{12}}{\rho} \right) \vec{n}_i \right) c_1 \vec{n}_i^T \right) = 0 \quad (31)$$

for the four direction vectors $\vec{n}_i = (\pm 1, \pm c_2/c_1)^T$. If we sum Eq. (31) for the two direction vectors $\vec{n}_i = (\pm 1, c_2/c_1)^T$ (i.e., we want to analyze the y -direction by “summing out” the x -direction) we obtain

$$\frac{1}{2} \left(v_1 \pm \frac{\sigma_{12}}{c_2 \rho} \right)_t \pm \nabla \cdot \left(c_2 \frac{1}{2} \left(v_1 \pm \frac{\sigma_{12}}{\rho c_2} \right) (1, 1) \right) = 0, \quad (32)$$

where the two signs indicate the two directions we did not sum over. For a 1-D problem

along the y -axis we now set $\nabla = (0, \frac{\partial}{\partial y})$ and obtain the correct 1-D advection equation along the y -axis (cf. Table I):

$$\frac{1}{2} \left(v_1 \pm \frac{\sigma_{12}}{c_2 \rho} \right)_t \pm c_2 \frac{1}{2} \left(v_1 \pm \frac{\sigma_{12}}{\rho c_2} \right)_y = 0. \quad (33)$$

Analogously one can sum over the y -direction and set $\nabla = (\frac{\partial}{\partial x}, 0)$ to obtain the correct advection equation along the x -axis. The other five components of our system can be treated in the same way. Thus, for a 1-D problem along the coordinate axis our scheme reduces to the exact 1-D transport of eigenvectors.

For plasticity we use the same idea. The only difference with elasticity is that we do not replace strain variables by stress variables in Eq. (6), which means instead of decomposing Eq. (30) we decompose the flux equation

$$\mathbf{V}_t + \nabla \cdot c \underline{\mathbf{L}} = 0$$

with

$$\underline{\mathbf{L}} = \frac{-1}{c} \begin{pmatrix} \frac{\sigma_{11}}{\rho} & \frac{\sigma_{12}}{\rho} \\ \frac{\sigma_{12}}{\rho} & \frac{\sigma_{22}}{\rho} \\ v_1 & 0 \\ 0 & v_2 \\ 0 & 0 \\ \frac{1}{2}v_2 & \frac{1}{2}v_1 \end{pmatrix}.$$

The wave model is exactly the same as that for elastic waves (cf. third column in Table II). The required stress update is discussed in the following section.

3.3. Stress Update

The Method of Transport we described previously yields an update for the strain and velocity vector contained in the vector \mathbf{V} at each time step. For purely elastic materials the stress variables can be calculated from the strains by their linear relationship (cf. [6]). However, for the update of the stress variables $\underline{\boldsymbol{\sigma}}$ in the plastic case one has to integrate the ODE (7) in time. The problem is that the strain variables $\underline{\boldsymbol{\epsilon}}$ are only known at discrete time levels t^n and t^{n+1} . However, to integrate Eq. (7) in time we have to know the derivative $\underline{\boldsymbol{\epsilon}}_t$ on the whole time interval $[t^n, t^{n+1}]$. Therefore, we reconstruct the strain path in time by polynomials in time:

$$\underline{\boldsymbol{\epsilon}}(\vec{x}, t) = \underline{\boldsymbol{\epsilon}}(\vec{x}, t^n) + \underline{\mathbf{a}}(\vec{x})(t - t^n) + \underline{\mathbf{b}}(\vec{x})(t - t^n)^2 + \dots \quad \forall t \in [t^n, t^{n+1}].$$

Since we can compute the time derivatives of the strain variables at time t^n and t^{n+1} by using

$$\frac{\partial}{\partial t} \epsilon_{ij}(t^*) = \frac{1}{2} \left(\frac{\partial v_j}{\partial x_i} + \frac{\partial v_i}{\partial x_j} \right) \quad (34)$$

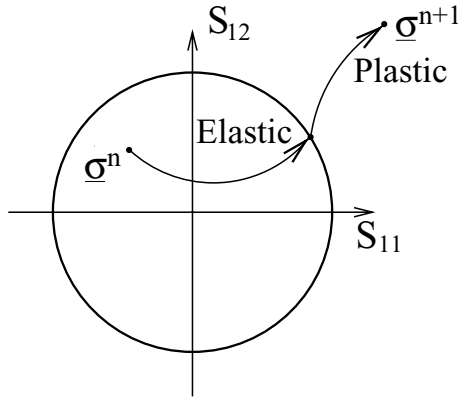


FIG. 2. Integration of the stress–strain relationship in the stress space from σ^n to the new state σ^{n+1} . The ODE solver has to be restarted on the yield surface (i.e., the level set of the yield function in the stress space separating elastic from plastic states) since the ODE can be discontinuous at the transition from elasticity to plasticity.

$$\frac{\partial^2}{\partial t^2} \epsilon_{ij}(t^n) = \frac{1}{2\rho} \sum_k \left(\frac{\partial^2}{\partial x_i \partial x_k} \sigma_{ik} + \frac{\partial^2}{\partial x_j \partial x_k} \sigma_{jk} \right) (t^n)$$

at $t^* = t^n$ or t^{n+1} (35)

(v_i is known at time t^n and t^{n+1} after the PDE time step and σ_{ij} is known at time t^n) we can reconstruct the strain variables up to order 4 and the time derivatives of the strain variables (and thus the right-hand side of ODE (7)) up to order 3.

Since we use third-order fluxes in the following numerical examples, it is sufficient to reconstruct the right-hand side of ODE (7) up to errors $\mathcal{O}(\Delta t^4)$ and using a high-order ODE solver (e.g., Runge–Kutta), the stress update will be of third order in smooth regions. However, any order can be achieved by using higher spatial derivatives analogous to (34).

With the help of this reconstruction one can integrate Eq. (7). It is important to note that during the integration a transition from elasticity to plasticity might occur where the right-hand side of the ODE is discontinuous. In such a case one has to find the exact transition point (e.g., by bisection or with Newton’s method) and then restart the ODE solver at this point (cf. Fig. 2).

4. NUMERICAL EXAMPLE FOR PLANE STRAIN

We consider two compression waves hitting a crack in a plate (cf. Fig. 3) under the previously described plane-strain condition. The physical parameters and initial conditions for the waves are chosen as

$$v_2^0 = 0.55, \quad \sigma_{22}^0 = \frac{v_2^0}{c_1}$$

$$c_1 = 1, \quad c_2 = \frac{1}{\sqrt{3}}$$

and the initial value for the yield parameter κ_0 is

$$\kappa_0 = 1 \quad \text{and} \quad \frac{\mu_p}{\mu} = \frac{3}{16}$$

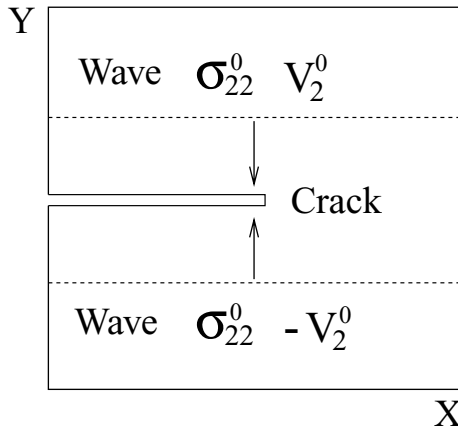


FIG. 3. Compression waves carrying the velocity $\pm v_2^0$ and the stress component σ_{22}^0 approaching a crack.

(the plastic shear modulus $\mu_p(\kappa)$ is assumed to be constant). The crack is simulated as a free boundary; i.e., the normal force and the boundary vanishes

$$\sigma \vec{n} = 0 \quad \text{with } \vec{n} \text{ denoting the surface normal.}$$

At first, one observes (cf. Fig. 4) two circular waves (*P*-wave and shear wave), which were created at the crack tip where the stress turns out to be singular. Furthermore, there is a von Schmidt wave (with wave speed c_2) created by the *P*-wave along the crack (it is a hypersonic wave) and a Rayleigh wave propagates along the surface of the crack. In addition to this

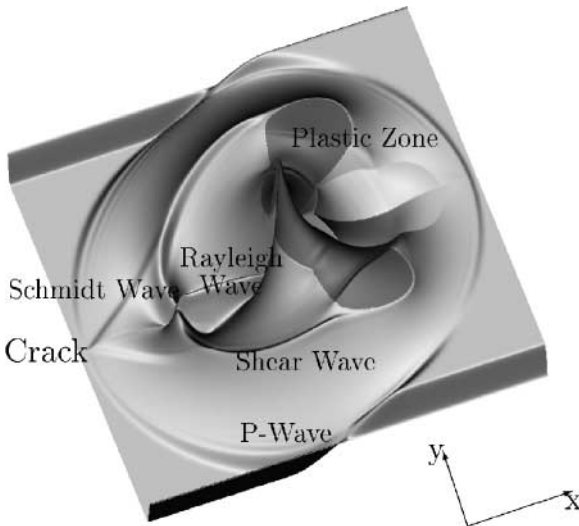


FIG. 4. Numerical computation of third-order of the maximal shear stress around the crack tip in the elastic case. The singularity created at the crack tip, the compression wave (=circular *P*-wave created at the crack tip propagating at c_1), the circular shear wave (propagating at $c_2 < c_1$), the Rayleigh wave (a wave propagating along the cracks surface), the von Schmidt wave (a conic wave created by the *P*-wave along the crack), and the plastic zone are well resolved (grid: 500×500 cells). The behavior of the waves is self-similar with respect to space/time.

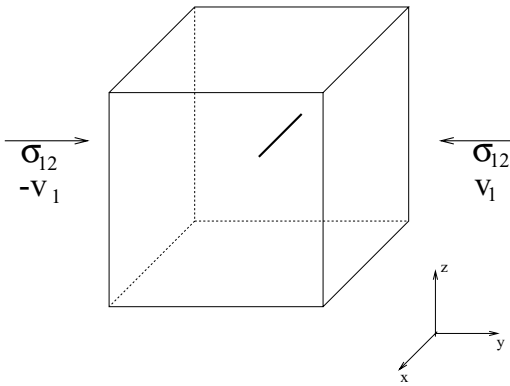


FIG. 5. One-dimensional crack in a body. From both sides of the crack, a plane wave propagates along the y -direction toward the crack. At time $t = 0$ both waves hit the crack.

physical behavior observed in the elastic region a zone of plastic deformation is created at the crack tip.

All physical effects one expects to appear around a crack tip are computed.

5. NUMERICAL RESULTS IN 3-D

The extension of our scheme to 3-D is straightforward. Instead of each component we have to use eight waves, each of which transport information at speed c_1 or c_2 as in the 2-D case (cf. Table II).

We consider a body in three space dimensions with a crack along the y -direction; i.e., all points in the set $M = \{(x, y, z)^T | y = 0, z = 1, \text{ and } 0 \leq x \leq 1\}$ are the crack. Analogous to the 2-D case a plane shear wave propagates along the y -axis toward the crack (cf. Fig. 5).

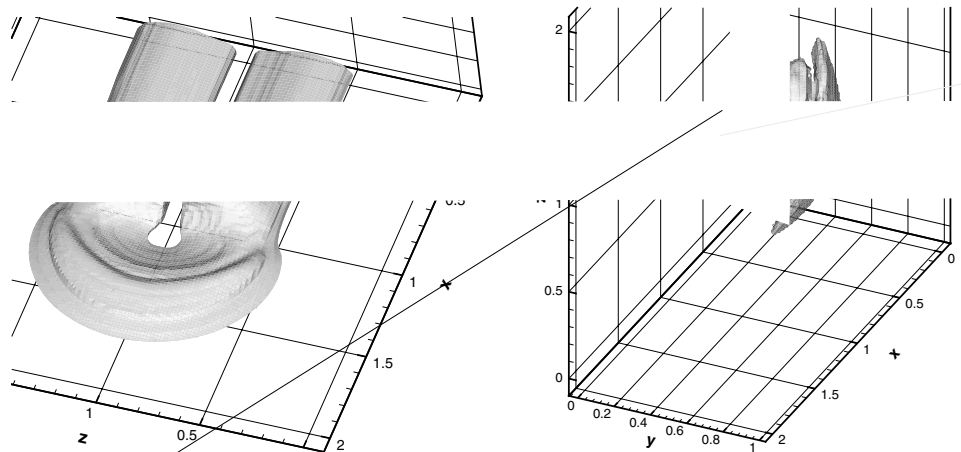
ve propagates along

ion is created at

omputed.

four waves \vec{n}_i in

direction; i.e., all



Both shear waves carry the stress and velocity component $\sigma_{12} = 0.5$ and $v_1 = -(\pm \frac{\sigma_{12}}{c_2})$, with the positive and negative sign indicating the positive and negative propagation direction along the y -axis. The wave speeds and the yield condition are chosen as in our previous 2-D example.

Figure 6 (left) shows the plastic zone created around the crack, which is a rather flat region on the x - z -plane. At the crack tip the stress turns out to be very intense. Furthermore, as in 2-D there is a spherical reflection created at the crack tip (cf. Fig. 6 on the right).

6. CONCLUSION

Although the elastic-plastic wave equation is not a pure conservation law, we could use the Method of Transport combined with a Runge-Kutta ODE solver to simulate plastic waves in solids in high order. The method we presented can be used up to any order in space (by reconstructing the solution by polynomials after each time step) and in time (by using correction terms in the numerical flux) and it can be used with any kind of hysteresis model, which can be described by an ODE at every point. Furthermore, Fey showed in [2, 3] that the Method of Transport can be used for nonlinear conservation laws, which shows that our method is not limited to the linearized model of small strains. Compared to other methods (cf. Introduction) the Method of Transport has the advantage that it can be implemented to any order in space and time and hence it allows high-resolution simulations with less computation time. Moreover, numerical experiments show that all kinds of physical effects known from textbooks, such as Rayleigh waves, von Schmidt waves, etc., can be simulated well.

REFERENCES

1. P. Colella, Multidimensional upwind methods for hyperbolic conservation laws, *SIAM J. Comput. Phys.* **87**, 171 (1990).
2. M. Fey, Multidimensional upwinding: Part I. The method of transport for solving the Euler equations, *J. Comput. Phys.* **143**, 159 (1998).
3. M. Fey, Multidimensional upwinding: Part II. Decomposition of the Euler equations into advection equations, *J. Comput. Phys.* **143**, 181 (1998).
4. M. Fey, R. Jeltsch, and A.-T. Morel, Multidimensional schemes for non-linear systems of hyperbolic conservation laws, in *Numerical Analysis*, edited by D. Griffiths and G. A. Watson (Longman, Harlow/New York, 1996).
5. M. Fey, R. Jeltsch, J. Maurer, and A.-T. Morel, The method of transport for nonlinear systems of hyperbolic conservation laws in several space dimensions, in *Proceedings of the Conference on Numerical Analysis, Zeist, 1996*.
6. P. L. Gould, *Introduction to Linear Elasticity* (Springer-Verlag, Berlin/New York, 1983).
7. D. Kröner, *Numerical Schemes for Conservation Laws* (Wiley-Teubner, New York/Leipzig, 1997).
8. R. J. LeVeque, *Numerical Methods for Conservation Laws*, Lectures in Mathematics (Birkhäuser, Basel, 1992).
9. X. Lin, *Numerical Computation of Stress Waves in Solids* (Akademie Verlag, Berlin, 1996).
10. X. Lin and J. Ballmann, Improved bicharacteristic schemes for two-dimensional elastodynamic equations. *Quart. Appl. Math.* **LIII**(2), 383 (1995).
11. X. Lin and J. Ballmann, A numerical scheme for axisymmetric elastic waves in solids, *Wave Motion* **21**, 115 (1995).

12. X. Lin and J. Ballmann, Numerical modelling of elastic-plastic waves in transversely isotropic composite materials, *ZAMM* **75**, 267 (1995).
13. X. Lin and J. Ballmann, Elastic-plastic waves in cracked solids under plane stress, in *Nonlinear Waves in Solids*, edited by J. L. Wegne and F. R. Norwood, ASME Book AMR 137 (1995), p. 155.
14. X. Lin and J. Ballmann, Numerical modelling of elastic-plastic deformation at crack tips in composite material under stress wave loading, *J. de Phys.* **III4**, S. C8-53 (1994).
15. J. Lubliner, *Plasticity Theory* (Macmillan Co., New York, 1990).
16. K. W. Morton and R. D. Richtmyer, *Difference Methods for Initial-Value Problems* (Krieger, Melbourne, FL, 1995).
17. W. K. Nowacki, *Stress Waves in Non-Elastic Solids* (Oxford-Pergamon, London/New York, 1978).
18. L. Prandtl, *Proceedings of the First International Congress for Applied Mechanics* (Delft, 1924).
19. D. Serre, *Systems of Conservation Laws* (Cambridge Univ. Press, Cambridge, UK, 1999).